ASEAN Engineering Journal

Full Paper

Computational Fluid Dynamics Analysis on Overweight Sleep Apnea Patient under Various Breathing Flow Patterns

Article history
Received
13 July 2022
Received in revised form
17 November 2022
Accepted
20 November 2022
Published online
31 May 2023

Muhammad Nooramin Che Yaakob[a,b], W.M.Faizal[a,*], C.Y. Khor[a]

[a]Faculty of Mechanical Engineering Technology, Universiti Malaysia Perlis, Perlis, Malaysia
[b]Department of Mechanical, Arau Vocational College, Perlis, Malaysia

*Corresponding author
wanmohd@unimap.edu.my

Graphical abstract

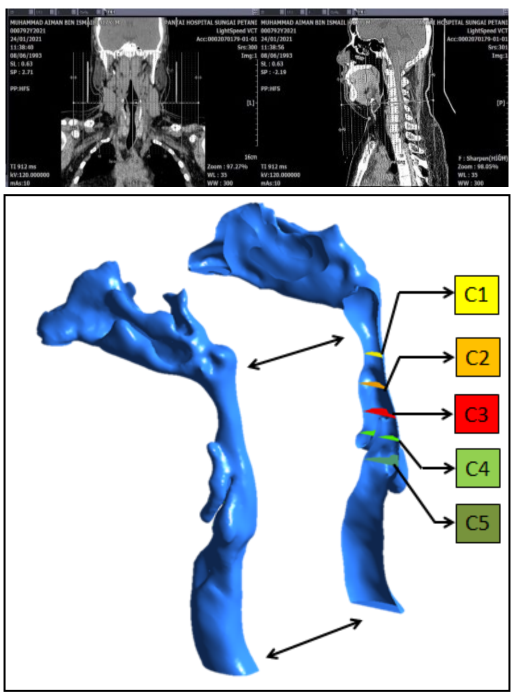

Abstract

Obstructive Sleep Apnea (OSA) is a breathing disorder that occurs during sleep. This syndrome affects numerous people, especially those with abnormal body fat composition parameters such as body mass index (BMI) of more than 25 kg/m^2 (overweight & obesity). OSA ensues when the tongue and soft palate muscles in a relaxed condition move towards gravity when the patient is in a supine position; this causes narrowing and blockage on the upper airway affecting breathing. There are several treatments for OSA, including upper airway surgery. A better understanding of airflow characteristics will assist ENT surgeons in identifying the blockage area. This paper examines airflow characteristics of the upper airway for overweight sleep apnea patients. The narrow and blockage area on the respiratory tract causes turbulence formation that is evaluated using Computational Fluid Dynamic (CFD) based on an actual parameter of the 3D model obtained by CT scan image result. Reynold's averaged Navier-Stoke (RANS) equation and turbulent model, k-ω shear stress transport (SST), were applied. Airflow fluctuation was characterized by crucial parameters such as velocity, pressure, and turbulent kinetic energy (TKE). The result shows that the narrow cross-sectional area of the airway causes accretion of the velocity and pressure in the pharyngeal airway. The increasing airflow parameter results in high turbulent kinetic energy (TKE) that will determine the severity level of OSA patients. Investigating airflow characteristics in overweight OSA patients will help the medical practitioner validate the narrow and blockage area for the surgery.

Keywords: Obstructive Sleep Apnea, Computational Fluid Dynamic, turbulent kinetic energy, Reynold's averaged Navier-Stoke

1.0 INTRODUCTION

The respiratory tract is divided into an upper and lower airway. It is a complex structure that plays an essential role during inhale and exhale breathing. The failure of the airway channel function in the upper airway will cause various diseases such as hypertension, myocardial infarction, cardiac failure, stroke, and cardiac dysrhythmias [1]. This respiratory tract problem, known as obstructive sleep apnea (OSA), often occurs during sleep. Benjafield AV et al. 2019 [2] have estimated that 425 million people worldwide have moderate to severe obstructive sleep apnea (OSA) between the ages of 30 to 69 years of age. The human upper airway (HUA) consists of the oral cavity, nasal cavity, pharynx, larynx, and trachea. When a person is in the supine position, the tongue muscles are relaxed; gravity pulls the tongue toward the back wall of the pharynx [3], as shown in Figure 1. The pressure on the pharynx's rear wall will affect the segment's cross-sectional area. Thus, it will cause breathing disorders during inhale and exhale breathing.

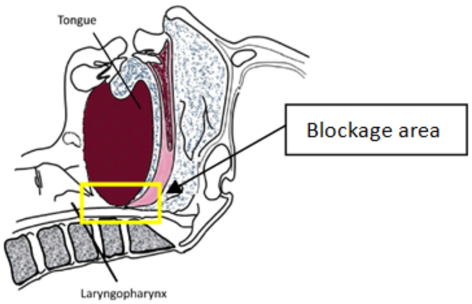

Figure 1: Tongue and soft plate muscle move towards gravity during supine position [3].

Several factors can increase the risk of OSA. The main contributing factor to OSA is obesity [4]. Multiple studies have identified overweight and obesity as critical risk factors for OSA development. Overweight and obese are strongly associated with OSA, with approximately 40%-70% of the obese population diagnosed with OSA [5]. The Caucasian population defined the value of body mass index (BMI) for obesity as more than 30 kg/m^2. Although, some Asian populations have redefined obesity from a BMI of 25 kg/m^2 [6]. The abnormal body fat composition, especially on the tongue muscle and the pharyngeal wall, will decrease muscle activity and lead to OSA [7]. According to Stephen H. Wang et al. 2019 [8], the obese patient will often cause developing fat on the tongue muscle. Thus the tongue enlargement due to the accumulation of fat on the tongue will narrow the cross-sectional segment on the upper airway, as shown in Figure 2.

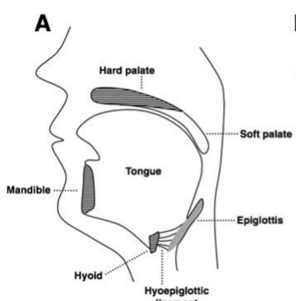

Figure 2 shows that tongue enlargement caused by fat composite will narrow the upper airway [8].

Hence, understanding the interaction between airflow with tongue and soft palate muscle is vital in investigating OSA flow characteristics for overweight sleep apnea patients. Since the narrowest segment and complex geometry of the pharyngeal airway, the air velocity in that region increases significantly and fluctuates. This flow pattern, called turbulent, will be examined via computational fluid dynamics (CFD) to solve and analyze the flow characteristic. Computational fluid dynamics (CFD) has been widely used in various fields, and one of them is the respiratory system due to its ability to provide detailed flow characteristics. The results are accurate and valuable compared to experimental and clinical observations [9]. The severity of OSA can be determined using Turbulence Kinetic Energy (TKE) by defining the behavior. Therefore, these studies investigate the effects of turbulent kinetic energy (TKE), velocity, and boundary wall pressure in the upper airway for overweight sleep apnea patients using computational fluid dynamics (CFD).

2.0 METHODOLOGY

2.1 Subject

The subject with a BMI of 28 kg/m^2 is selected to investigate the flow characteristics of overweight sleep apnea patients. The subject has OSA symptoms such as loud snoring, insomnia, awakening with a dry mouth, and morning headache. Thus, the subject has been chosen to undergo subsequent studies. Table 1 is shown the details of the subject selected:

Table 1 Subject details.

Subject physical data	
Age	27
Gender	Male
Weight	81 kg
Height	170 cm
BMI	28 kg/m^2

2.2 CT Scan Data Of Human Upper Airway

The 3D model is a crucial part of the computational fluid dynamics method. All the parameters in the 3D model geometry should be accurate to avoid inaccurate simulation results. Thus, there are several proses to create a 3D model of the human upper airway based on the CT scan image. Referring to the patient CT scan image result obtained, the occurrence of a narrowing segment of the pharyngeal airways on cross-section area A-A (oropharynx area), which is 57.183 mm^2, as shown in Figure 3.

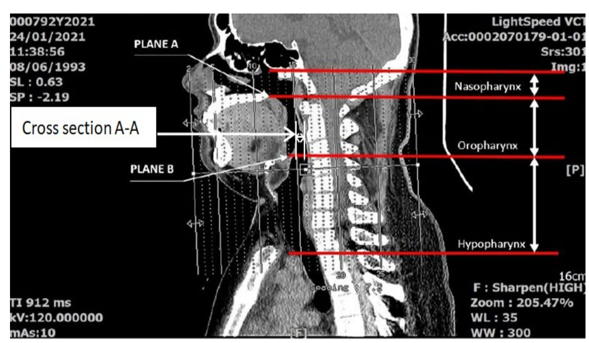

Figure 3: The narrowness of the pharyngeal airways in the oropharynx area (Cross-section A-A).

According to Ogawa et al. (2007) [10], their studies prove that the minimum cross-section area of the pharyngeal airway for OSA patients is 45.8±17.5 mm^2, while Non-OSA is 146.9±111.7 mm^2.

2.3 Converting Surface Geometry To Volume Geometry

MIMICs are image processing software for 3D design and modeling. Based on patient results from CT scan images, the data in DICOM (*.dcm) file format was imported to MIMICs to analyze the parameters and merge all axial, coronal, and sagittal scan images into a single volume file project. MIMICs will compile all individual 2D images (cross-sections) and match all the coordinates. Then, each view's coordinates are synchronized. The patient data on MIMICs is shown in Figure 4.

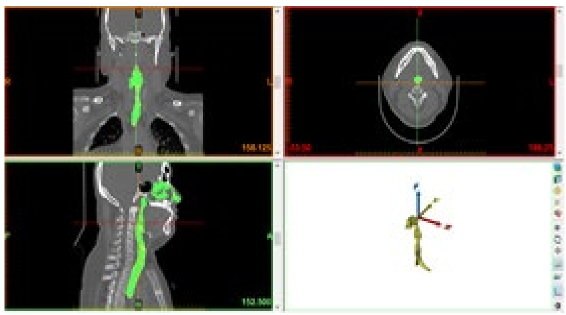

Figure 4: The coordinates of each view are synchronized on a particular area.

The 3D surface model was accomplished by defining a threshold value range and creating a segmentation mask. The threshold value is used to discriminate different electron densities. In the human upper airway, CT scan images show the airway channels appear black; surrounding airway tissues appear grey. The 3D anatomical model of the upper airway was created based on a segmented mask in MIMICs. The 3D upper airway model was examined using 3D rendering tools to ensure that the threshold was suitable and all necessary structures were present. After completing the 3D surface structure of the upper airway using MIMICs, export the data file in IGES format. 3D volume geometry of the upper airway will create via SOLIDWORK, Cad modeling.

2.4 Meshing Of Human Upper Airway 3D Model

The 3D model reconstruction of the upper airway geometry was exported to Hyperwork & Hypermesh, Altair, for model trimming and mesh generation. The meshing quality will influence the simulation's accuracy, convergence, and duration. Thus, a grid independence test was conducted to choose the best mesh element to simulate. Initially, 1.73 million elements are generated in the human upper airway 3D model—the selected mesh element parameters as shown in table 2.

Table 2: Mesh element parameters.

Mesh Element	Value
Volume statistics:	
minimum volume (m^3)	1.831x10^-5
maximum volume (m^3)	0.270x10^-1
Face area statistics:	
minimum face area (m^2)	7.183x10^-4
maximum face area (m^2)	9.407x10^-1
Maximum deviation	0.2
Growth rate	1.3

To ensure the mesh quality is achieved, the average skewness and standard deviation value were considered [11]. The mesh 3D model upper airway is shown in Figure 5.

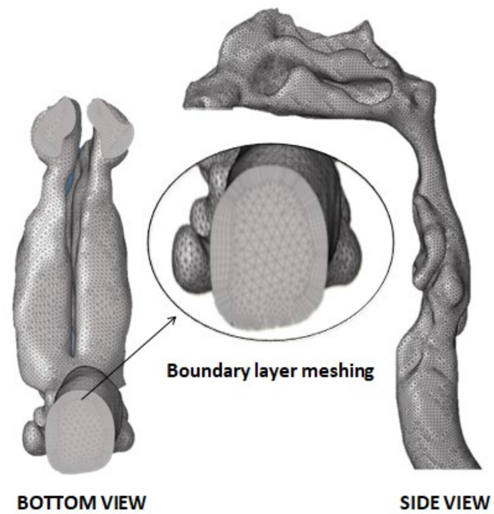

Figure 5: 3D Model Of Upper Airway Meshing.

The 5-grid layer size was used for grid sensitivity test results based on establishing acceptable accuracy. The accuracy of grid size was proven by the prior research approach by Jeong & Sung (2007) [12].

2.5 Simulation Modeling

A simulation is the execution of a model, represented by a computer program that gives information about the investigated model. The upper airway model that has been designed will be analyzed using computational fluid dynamic (CFD) ANSYS Fluent. The simulation approach to analyzing a model is opposed to the analytical method. The turbulent flow created by narrowing pharyngeal airways for overweight sleep apnea patients will examine by Reynolds Average Navier-Stokes (RANS) equation and using k-ω SST as a turbulent model, simulated via CFD solver. The results were explained by the Turbulent Kinetic Energy (TKE) to visualize and analyze the airflow characteristics to determine the severity of OSA.

2.6 Governing Equation

Regional flow patterns differ according to subject geometry, such as narrow and complex structures [13]. The continuity and Navier-stokes equations are fundamental governing equations describing the upper airway's flow characteristics. The Navier-Stokes (N-S) equation is the broadly applied mathematical model to examine changes in those properties during interactions. The equations are adjustable regarding the content of the problem and are expressed based on the principles of conservation of mass, momentum, and energy. In recent studies, the steady-state solution of the airflow in the pharyngeal airway is assumed incompressible due to the airflow being in the lower velocity range [14], and fluid temperature is constant due to temperature change in the respiratory tract is a slight difference. The governing equations for the airflow in the pharyngeal airway are given as follows:

Continuity equation

$$\nabla \vec{v} = 0 \tag{1}$$

Momentum equation

$$\rho(\vec{v} \cdot \nabla) = \rho \vec{g} - \nabla \rho + \mu \nabla^2 \vec{v} \tag{2}$$

The continuity and momentum equation defines the flow characteristic and calculates the velocity and airflow pressure. Reynolds-averaged Navier–Stokes (RANS) equation is used to solve the turbulent flow in the upper airway. The equation is given as follows:

Reynolds-averaged Navier–Stokes (RANS)

$$\rho u_i \frac{\partial u_j}{\partial x_i} = -\frac{\partial P}{\partial x_i} + \frac{\partial}{\partial x_i}\left[\mu\left(\frac{\partial u_i}{\partial x_j} + \frac{\partial u_j}{\partial x_i}\right) - \rho\overline{u_i' u_j'}\right] \tag{3}$$

The model k-ω SST is used to calculate the Reynolds stress $(= -\rho\overline{u'_i u'_j})$.

The Turbulent Kinetic Energy (TKE) represents the average kinetic energy per unit mass associated with the recirculation zone in a turbulent flow. The kinetic energy of turbulence is characterized by measured root-mean-square (RMS) velocity fluctuations. Using the Reynolds decomposition method, the velocity signal *u* is separated into a mean component *u* and a fluctuation component *u'* [15]. Thus, the value of turbulence fluctuation is described by root-mean-square (RMS) as:

$$u' = \sqrt{\frac{1}{N_i}\sum_{i=1}^{N}(u_i - \bar{u})^2} \tag{4}$$

The value N is the number of measurements. Thus, Turbulence Kinetic Energy (TKE) can be defined as:

$$TKE = \frac{1}{2}\rho(u'^2 + v'^2 + w'^2) \tag{5}$$

Where *u'*, *v'*, and *w'* are the fluctuating velocity components, and ρ is the density.

The complicated airflow in the pharyngeal airway is analyzed using turbulent models, Eddy Viscosity Model (EVM), and Reynold Stress Model (RSM), which are utilized to simulate the airflow characteristics. The solution selection for the turbulence model depends on various scales and combinations of distinct flow mixes or phases. The RANS model with two equations is suggested for the HUA simulation inquiry. According to prior research, the SST k–ω model generated reliable findings and saved simulation time compared to other turbulent models to investigate turbulent flow in the human upper airway [16]. While Reynolds Stress Model (RSM) provides excellent results with complex flows, it requires more CPU effort and takes longer simulation. Besides, RMS is more difficult to converge than the 2-equation models and is most suitable for complex 3D flows with strong streamlines. Thus, to investigate turbulent flow in the human upper airway, the turbulent model SST k–ω is the most suitable turbulent model to analyze the airflow characteristics in the human upper airway (HUA).

2.7 Boundary Condition

Boundary conditions implemented for the computational fluid dynamic (CFD) simulations include mass flow rate as an inflow boundary condition and no-slip condition for the airway walls (control volume is fixed). ANSYS Fluent simulated the 3D model in steady-state turbulent airway flow, and 10% of the turbulent intensity was considered sufficient to mimic the actual conditions. The outlet was defined by an average gauge pressure of 0 Pa [14]. The air properties of the simulation model as shown in Table 3.

Table 3: Air properties

Air properties	
Air Density (ρ)	1.225 kg/m^3
Dynamic Viscosity (μ)	1.789x10^{-5} kg/ms
Kinematic Viscosity (v)	1.5111x10^{-5} m^2/s

The airflow in the pharyngeal airway is assumed incompressible due to the airflow being in the lower velocity range [17]. There are few computational investigations of heat and moisture transmission in the upper airway of humans. They assume a constant moisture and temperature in human upper airway [18]. Besides, according to M. Faizal et al., 2021, the fluid temperature, T, is assumed constant because the temperature changes within the human airway are minimal (32◦C ±0.05◦C).

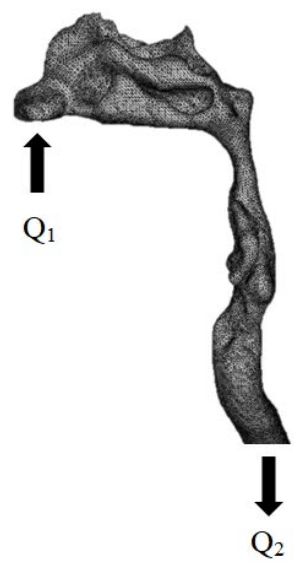

Figure 6: The airflow direction during inhaled breathing.

Figure 6 shows the flow inlet, Q1, on the nasal choanae level, and the velocity direction is perpendicular to the surface profile. The velocity profile was assumed to be uniform, and the axial component of the velocity was vertical to the flow inlet, nasopharynx [15]. The six mass flow rate values are used to analyze steady-state airflow by various inlet velocities (Table 4). The minimum flow rate is 6 L/min, a light breathing condition [19], while the maximum flow rate is 36 L/min [20]; heavy breathing is used in the simulation. The opening profile 3D model geometry allows the airflow through the boundary; therefore, the inlet section of the boundary is specified by atmospheric pressure ($P_{inlet} = P_{atmo}$: Gauge pressure is 0 Pa). Because the flow pressure change within the nasal cavity is relatively minor (approximately 10%) than within the pharyngeal airway, the atmospheric pressure was applied at the inlet boundary [21].

Table 4: Mass flow rate.

	Mass Flow rate
CASE 1	6 L/min
CASE 2	12 L/min
CASE 3	18 L/min
CASE 4	24 L/min
CASE 5	30 L/min
CASE 6	36 L/min

3.0 RESULT

3.1 Airflow Velocity In Pharyngeal CFD Model

The present study investigated the airflow in the pharyngeal airway that has been disturbed by a narrow cross-section segment. The airflow velocity is affected by narrow areas [22]. Five cross-sections have been identified to analyze the airflow pattern in detail, as shown in Figure 7.

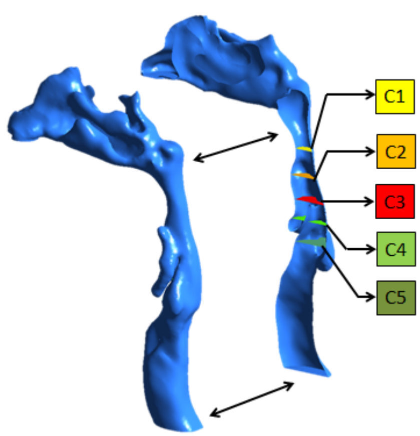

Figure 7: Cross-section C1-C5 in pharyngeal airway.

The cross-section C1 is located in the velopharynx area; C2, C3, and C4 are on the oropharynx, while C5 is on the laryngopharynx. Figure 8 shows the region of the cross-section segment of C1-C5.

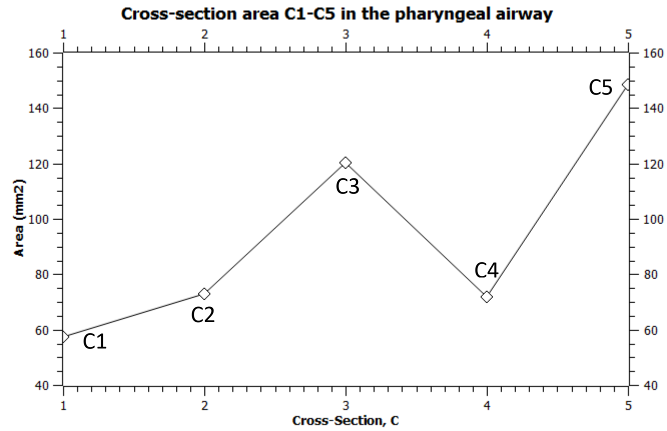

Figure 8: Area of cross-section C1-C5.

The various mass flow rates are used to visualize the flow characteristic. The results show that during inhalation, the increase in mass flow rate will increase velocity in the pharyngeal airway (Figures 9 & 10). The problem was calculated using the k–ω SST turbulence model. Based on the contour plot, cross-section C4 is a higher velocity for each case. The oropharynx region (C2, C3, C4) is a critical area compared velopharynx (C1) and laryngopharynx region (C5). For low inhalation cases 1, 2, and 3 (Figure 9), the maximum velocity on contour plot C4 for each case is $C4_1$=12.163 ms^{-1}, $C4_2$=26.042 ms^{-1}, $C4_3$= 40.146 $ms^{-1,}$ showing there is a slight increase due to increasing of mass flow rate. However, during heavy breathing for case 4, 5, and 6 (Figure 10), the structural geometry of the pharyngeal airway play a dominant role in causing the fluctuation of velocity. Thus, the narrow and complex structure area of the oropharynx region increases the velocity. As a result, the velocity increases from C2 to C4, and the higher velocity is on C4.

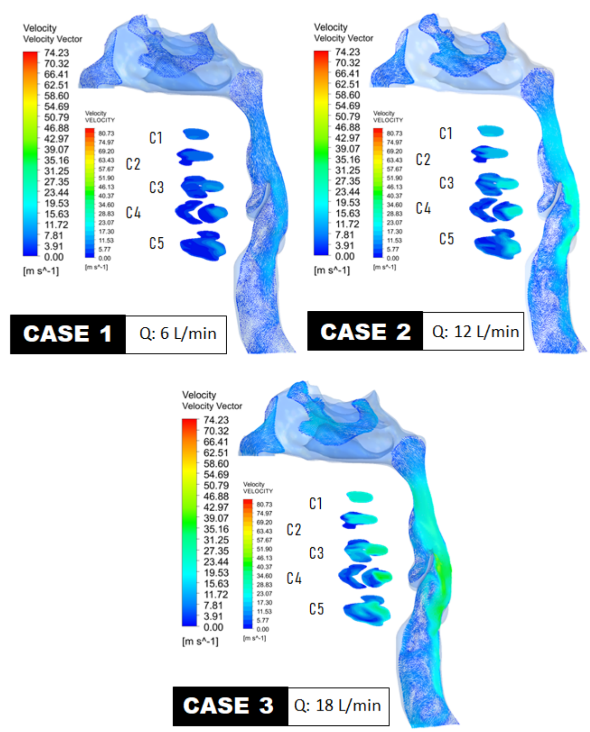

Figure 9: Velocity vector & contour during low inhale breathing.

The maximum velocity for cases 4, 5, and 6 on contour plot C4 is $C4_4$= 52.408 ms^{-1}, $C4_5$= 67.368 $ms^{-1,}$ and $C4_6$= 80.382 ms^{-1}.

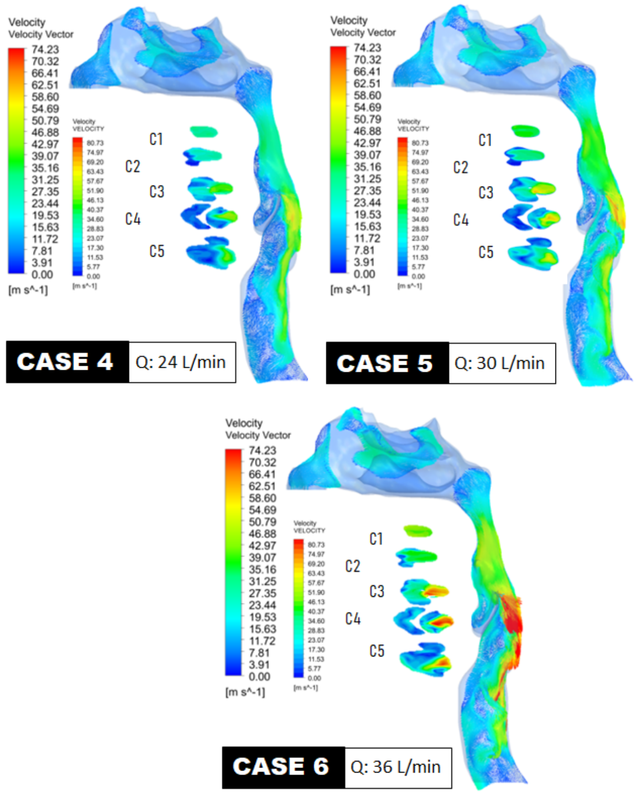

Figure 10: Velocity vector & contour during heavy inhale breathing.

The fluctuation of velocity is caused by complex structures and different cross-sectional areas in the pharyngeal airway. The CFD result shows the velocity distribution on C1 to C5, while C4 is the highest velocity among the other contour plots. Table 5 shows the maximum velocity on the contour plan in the pharyngeal airway for each case.

Table 5: Velocity distribution on C1, C2, C3, C4, and C5.

	CASE 1	CASE 2	CASE 3
C1	8.831 ms^{-1}	17.498 ms^{-1}	24.772 ms^{-1}
C2	8.173 ms^{-1}	15.139 ms^{-1}	24.241 ms^{-1}
C3	11.776 ms^{-1}	23.371 ms^{-1}	32.566 ms^{-1}
C4	12.163 ms^{-1}	26.042 ms^{-1}	40.146 ms^{-1}
C5	11.872 ms^{-1}	23.173 ms^{-1}	32.043 ms^{-1}

CASE 4	CASE 5	CASE 6
35.382 ms^{-1}	36.801 ms^{-1}	48.307 ms^{-1}
27.478 ms^{-1}	32.216 ms^{-1}	39.243 ms^{-1}
46.072 ms^{-1}	50.421 ms^{-1}	55.235 ms^{-1}
52.408 ms^{-1}	67.368 ms^{-1}	80.382 ms^{-1}
47.245 ms^{-1}	54.315 ms^{-1}	65.412 ms^{-1}

The narrow area on cross-section A-A, as shown in Figure 3, generates high-speed velocity and fluctuated airflow and causes turbulence in the oropharynx region (C2, C3, and C4). The result shows that the mass flow rate value will affect the airflow characteristic, such as air velocity, as shown in Figure 11. The mass flow rate increase will increase air velocity value depending on the cross-sectional and complex area of the pharyngeal airway.

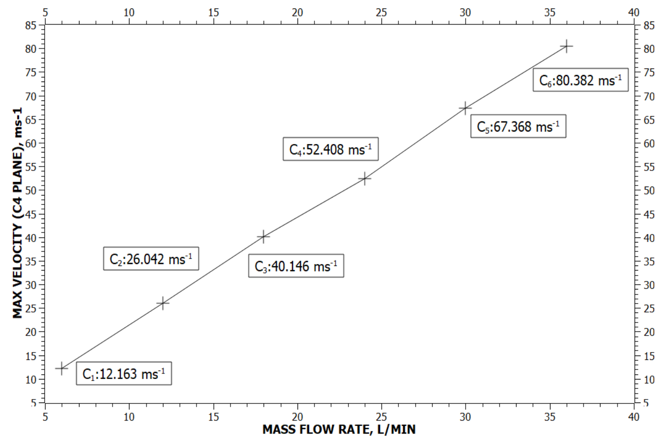

Figure 11: Maximum velocity for cases 1-6.

Thus, the results show that the high mass flow rate in case 6 generates the highest velocity in the oropharynx region. The fluctuation of airflow in the oropharynx region is obviously can see in case 6, as shown in Figure 12.

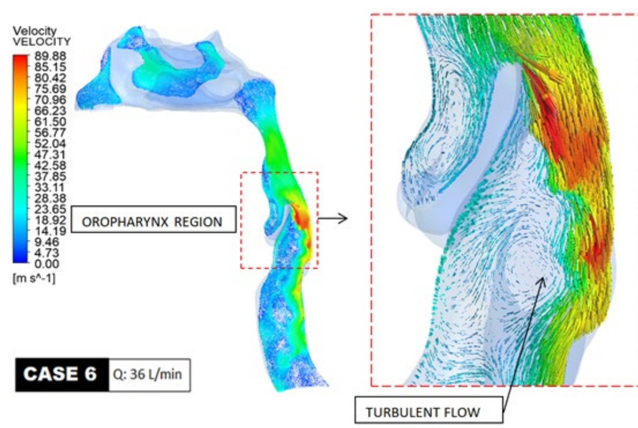

Figure 12: Turbulent flow in the oropharynx region.

The main contributor to the turbulence flow is the narrow area, high mass flow rate, and complex geometry of the pharyngeal airway. The fluctuated velocity (turbulent) will investigate using Turbulence Kinetic Energy (TKE).

3.2 Pressure On A Pharyngeal Wall CFD Model

The high-pressure regions occur at the edges of the nasal cavity. In contrast, the low-pressure areas have occurred at the nasopharynx, oropharynx, and hypopharynx, as shown in Figure 11. The pressure is comparatively high near the inlet and gradually decreases if the airflow velocity increases due to the narrow segment of the pharyngeal airway.

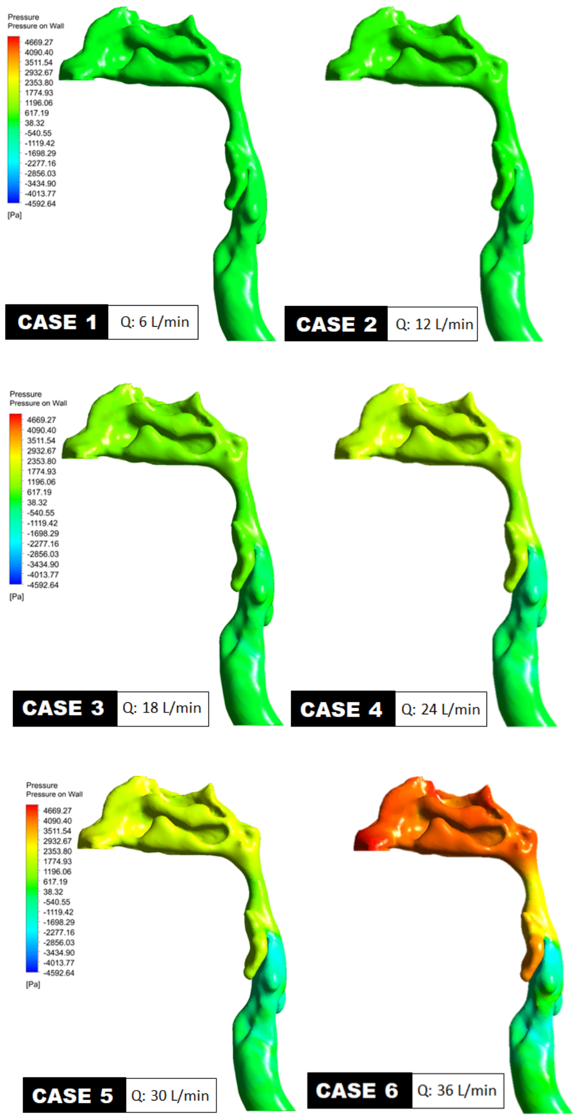

Figure 13: Pressure contour during inhale breathing.

Based on CFD simulated results, the maximum pressure occurs at the nasopharynx area, which obviously can be seen in case 6, where the maximum pressure on the wall is 4777.36 Pa. The increasing mass flow rate during inhale breathing causes an increase in pressure on the pharyngeal airway, as shown in Figure 13. For cases 1, 2, and 3, the pressure on the wall is below 1 kPa. Nevertheless, when the mass flow rate increases for cases 4, 5, and 6, the an apparent change in pressure contour. The highest pressure is spotted at the nasopharynx, and the lowest pressure is spotted on the hypopharynx. However, when the mass flow rate increases, the pressure contour increases on the oropharynx—the details of pressure distribution as shown in Figure 13. According to Figure 9, the oropharynx region is a higher velocity magnitude due to a narrow cross-section in the laryngeal region (minimum cross-section). The narrow cross-section area is created a laryngeal jet that causes rapid acceleration [23]. The laryngeal jet cause fluctuated airflow that decreases the pressure and increases the velocity magnitude. As a result, shown, the airflow passing through the minimum cross-section area (laryngeal region) reduces the pressure on the oropharynx region. The minimum pressure on the oropharynx region for each case is C_1=40.10 Pa, C_2=203.92 Pa, C_3=485.56 Pa, C_4=965.736 Pa, C_5=948.312 Pa, and C_6=2955.48 Pa.

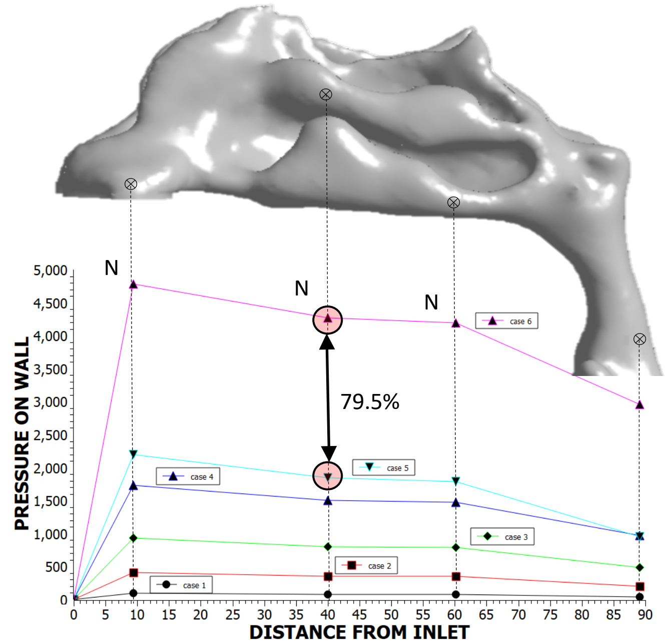

Figure 14: Pressure distribution for cases 1 to 6.

Based on the CFD simulated result, the mass flow rate will constantly increase the pressure on the upper airway wall. However, pressure for case 6 (36 L/min) is drastically increased, as shown in Figure 14. The increment in pressure percentage for case 5 and case 6 on the nasopharynx, N_2 is 79.5%, and pressure drops in the hypopharynx region. According to Bernoulli's principle, the pressure drop is due to increased velocity.

3.3 Reynolds Number

The Reynolds number describes flow patterns in laminar or turbulent flow (Eq.4).

$$Re = \frac{Inertia\ Force}{Viscosity\ Force} = \frac{\rho D \bar{u}}{\mu} \qquad (6)$$

Where ρ is the density, D is diameter, u is the flow speed, and μ is the dynamic viscosity

When the Reynolds number is low, the viscous force has a more significant impact on the flow field than the inertia force, and velocity disturbances in the flow field are attenuated due to viscous force, resulting in steady and laminar fluid flow. In contrast, when the Reynolds number is large, the influence of inertia on the flow field is greater than that of viscous force, fluid flow is more unstable, and it is simple to create and amplify small changes in velocity, resulting in a chaotic and irregular turbulent flow field [24]. According to this study, the shapes of five cross-sections of the upper airway are varied and irregular; as a result, their *Re* values will vary during the whole flowing process. The increasing diameter size/cross-sectional plane will increase the Reynolds value. As shown in figure 15, the Reynolds number for each case cross-section plane is fully turbulent with Re>4000.

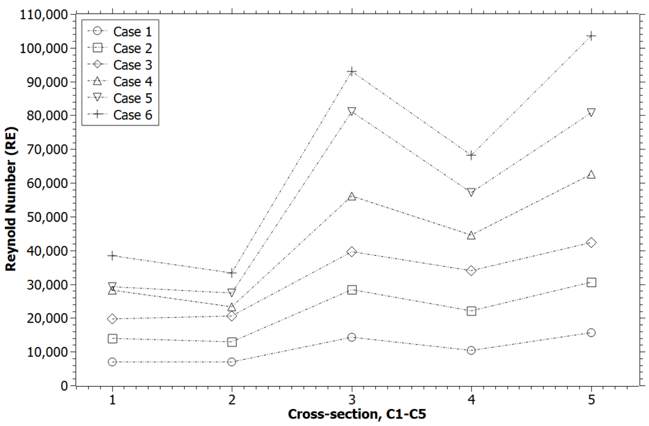

Figure 15: Reynolds number of different cases based on Eq. (6)

The Reynolds number increased dramatically with the increase in mass flow rate. As seen in Figure 15, the Re for case 1 is lower than other cases with the minimum Re on cross-section, C1 with the Reynolds value is *Re*=7032 (turbulent condition). Thus, the airflow along the human upper airway through all cross-section planes is in turbulent condition.

3.4 Turbulent Reynolds number

In the present work, the turbulent Reynolds number was investigated to explain the energy of the Reynolds number. In contrast, the Reynolds value determines the flow condition, either laminar or turbulent. The turbulent Reynolds number is expressed in Eq. (7). The turbulent Reynolds number is used to analyze the turbulence stage in the human upper airway for each case 1-6. The rising of the turbulent Reynolds number demonstrates airflow fluctuation with high kinetic energy and less work of friction in the human upper airway. The turbulent Reynolds number simulation result for low and heavy breathing is shown in figure 16.

$$Re_y = \frac{Kinectic\ Energy}{Work\ of\ friction} = \frac{KE}{W} \quad (7)$$

Where KE is kinetic energy, and W is the working friction force.

Based on the result obtained was shown the maximum turbulent Reynolds number is on the cross-section plane, C5, for each case. The highest Re_y is in case 6 on the cross-section plane, C5, with Re_y= 66904. According to figure 17, was shown Re_y increase dramatically when passing through the cross-section plane, C4. The Re_y is obviously can see on the cross-section plane, C5. The result indicates less work friction and high kinetic energy on plane C5 increase the Re_y. However, the result of the turbulent Reynolds number does not describe details on airflow characteristics. Thus, the investigation of Turbulent Kinetic Energy (TKE) for each case will give concentration and strength of the turbulence. The TKE is an important variable for measuring the intensity of turbulence.

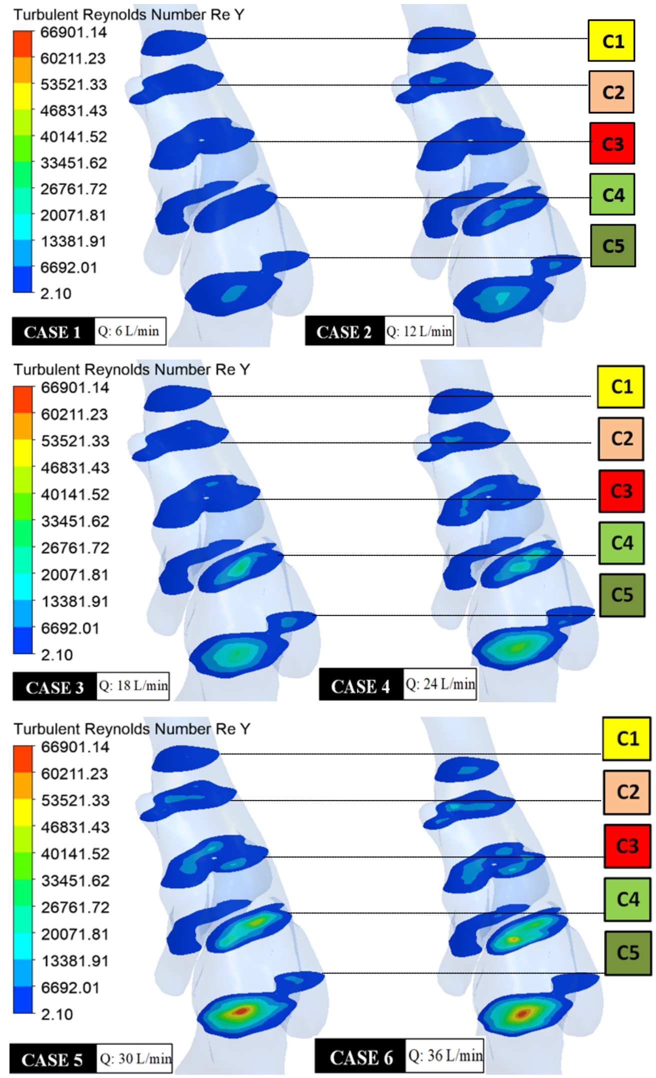

Figure 16: Turbulent Reynolds Number of different cases

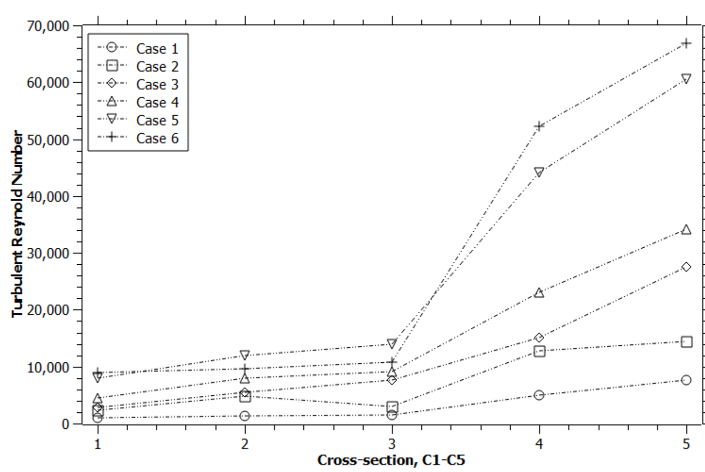

Figure 17: Turbulent Reynolds Number of different cases

3.5 Turbulent Kinetic Energy (TKE)

The turbulence is identified by the velocity fluctuation and is defined in terms of turbulence kinetic energy (TKE) [25]. The increasing turbulence intensity will generate more kinetic energy that transforms into turbulent kinetic energy [26]. The severity of obstructive sleep apnea (OSA) is recognized using TKE. The TKE describes the airflow characteristic in the upper airway. The contours of the TKE CFD result are shown in Figure 18 for cases 1 to 6.

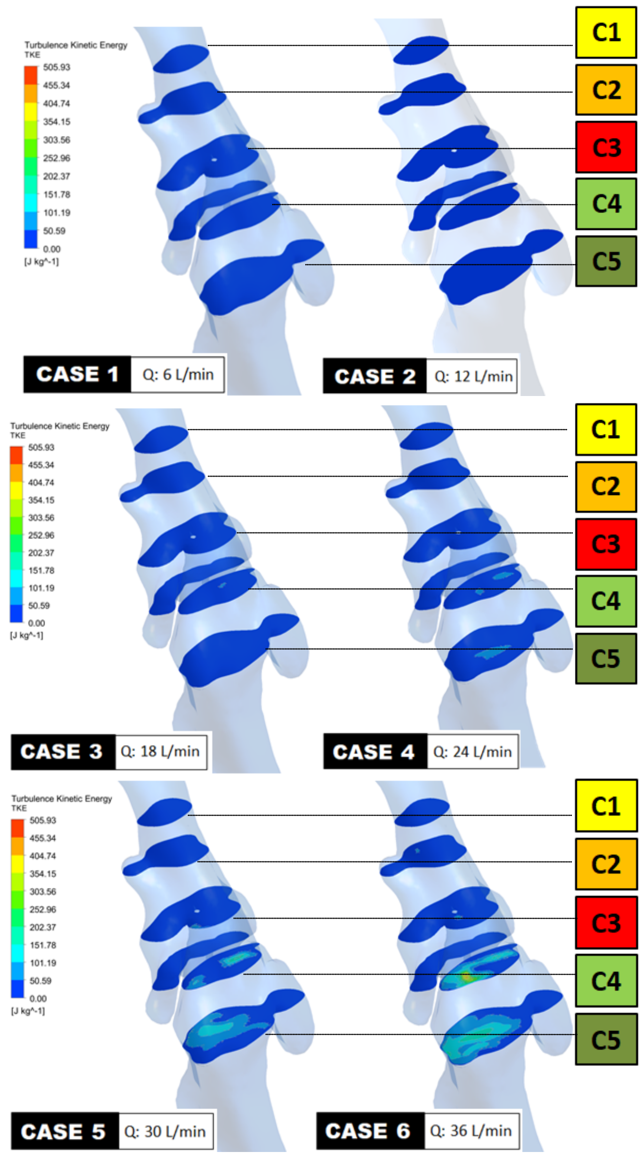

Figure 18: TKE contour on cases 1 to 6.

The distributions of turbulent kinetic energy (TKE) are shown in cross-sections C1 to C5. The fluctuation of velocity in the pharyngeal airway will create TKE. The high TKE spotted on cross-section plane C4, the value TKE cross-section plane C4 for each case is C_1= 2.178 J kg^{-1}, C_2= 17.560 J kg^{-1}, C_3= 63.509 J kg^{-1}, C_4= 90.283 J kg^{-1}, C_5= 187.213 J kg^{-1}, C_6= 505.93 J kg^{-1}. Based on the CFD result, the increase of TKE is related to high mass flow rate intake. However, the main crucial for increasing TKE is the cross-section area and complex structure of the pharyngeal airway. Figure 12 shows that high fluctuation velocity occurs in case 6 in cross-section C4. The high turbulent velocity in the oropharynx region will create high turbulent kinetic energy (TKE) and cause vibration in the surrounding area. According to Figure 19, the airflow passing through the narrow cross-sectional area dramatically increases the TKE due to velocity fluctuation. The airflow characteristic can see in case 6 (36 L/min) with the highest TKE value on the C4 plane.

4.0 DISCUSSION & CONCLUSION

During inspiration, the velocity rises from near zero at the nostrils to the maximum in the oropharynx region. In the narrow area (plane, C4), a high-velocity jet, higher turbulent kinetic energy, and pressure drop can be detected. Figure 19, 20 and 21 show the relationships between velocity, pressure, and Turbulent Kinetic Energy (TKE).

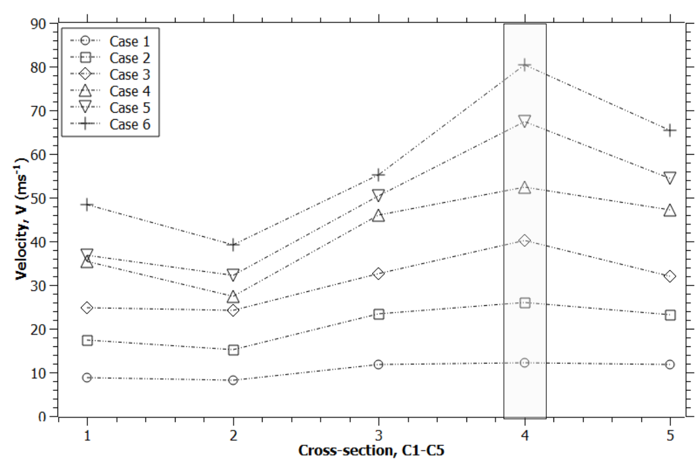

Figure 19: Velocity distribution along cross-section plane C1-C4.

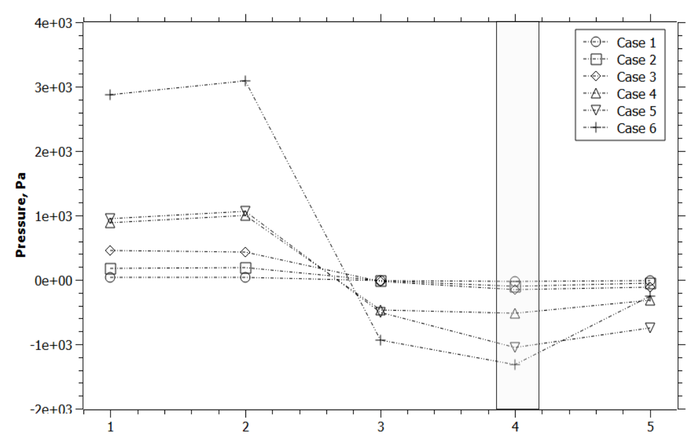

Figure 20: Pressure distribution along cross-section plane C1-C4.

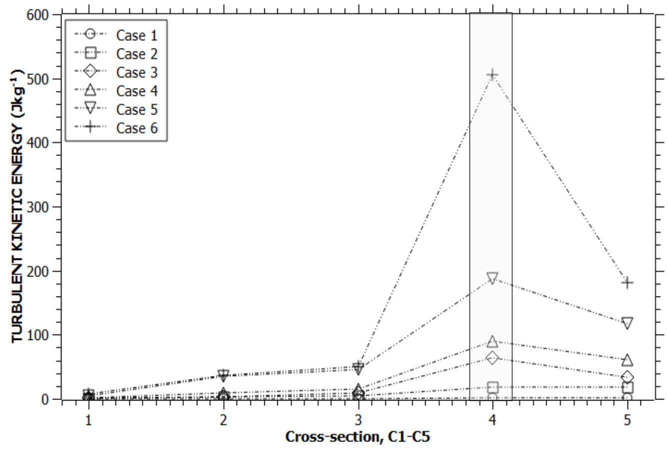

Figure 21: Turbulent Kinetic Energy (TKE) along cross-section plane C1-C4

Figures 19 and 21 show the airflow's velocity and turbulence kinetic energy are relatively high when the airflow is at the cross-section C4 (oropharynx region). The increasing value of velocity and TKE is due to the impact of the laryngeal jet on the respiratory tract wall and the vortices generated from the complex geometry. Besides increasing velocity on the cross-section plane, C4 will decrease the pressure. The present study proved that OSA's major contributions are caused by increasing velocity, turbulent kinetic energy, and pressure drop. Therefore, based on the result obtained, the most affected region is on the cross-section plane, C4 (Figure 22).

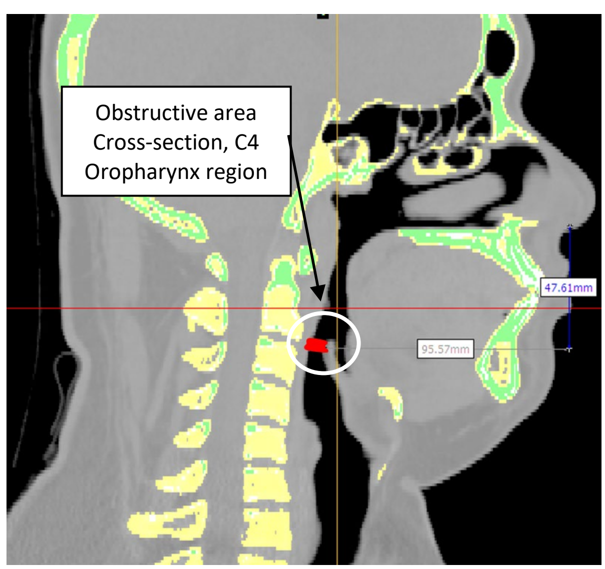

Figure 21: Obstructive on cross-section, C4 region

Many researchers have proved the effects of the narrow cross-sectional area on airflow characteristics. Ogawa et al. (2007) [10], in their research *'Evaluation of Cross-section Airway Configuration of Obstructive Sleep Apnea,'* prove that the narrow cross-sectional area due to obesity/overweight causes OSA. In their study, ten subjects with OSA and Non-OSA were selected the patients parameters was shown in Table 6. All subjects had polysomnographically confirmed OSA, with a mean Apnea/Hypopnea Index (AHI) of 23.4 and a standard deviation of 9.59. Non-OSA does not have any history of snoring or sleep apnea symptoms. This study evaluated the 3D images obtained by a dentomaxillofacial volumetric imaging system [10]. Based on the result, the range of cross-sectional area cause of OSA is 45.8 $mm^2 < OSA < 63.3\ mm^2$.

Table 6: OSA patients parameters [10].

	OSA AVE. SD
Gender	F=2, M=8
Age	52.9±14.7
BMI (kg/m^2)	29.5±9.05
Volume (mm^3)	4868.4±1863.9
Smallest Area (mm^2)	45.8±17.5
AP (mm)	4.6±1.2
L (mm)	11.6±4.5
AP/L	0.39±0.26
Location	UO=3, LO=7

Besides numerical method studies, Guo et al., 2020 [27], in their research regarding *A steady-state numerical investigation*, showed the effects of high velocity and TKE on the human upper airway. The high value of TKE creates a vibration in the surrounding area and causes snoring. Therefore, velocity, pressure, and TKE are essential for examining the flow characteristics of OSA patients and determining the severity of OSA.

In conclusion, the main findings from the study can be summarised as follow:

- The mass flow rate increase will affect the pressure, velocity, and turbulent kinetic energy (TKE) value. The result is shown in Figures 18, 19 &20.
- The velocity increases through a narrow cross-sectional area will create fluctuating airflow in the oropharynx region depending on the value of the inlet mass flow rate. The increase in mass flow rate has shown changes in significant parameters.
- The obstructive area created a laryngeal jet, causing fluctuation velocity to increase the turbulent kinetic energy (TKE) (Figure 12).
- High pressure occurs in the nasopharynx region, and lower pressure in the hypopharynx region. The different pressure values appear on the cross-section plane; C1-C5 and C4 plane is the lowest pressure.
- Increasing turbulent kinetic energy (TKE) created a vibration in the surrounding area and caused snoring.
- Overweight and obese cause a narrow cross-sectional area in the pharyngeal airway and contributes to OSA.

Acknowledgement

This work is supported by the Fundamental Research Grant Scheme provided by the Ministry of Higher Education (Ref. No. FRGS/1/2020/TK0/UNIMAP/03/26)

References

[1] Kushida, C.A., Culebras, A., Ivanenko, A., Watson, N.F., 2007. Obstructive sleep apnea: Pathophysiology, comorbidities, and consequences. New York, N.Y: Library of Congress Cataloging-in-Publication Data. 3(1):1-3. DOI: https://doi.org/10.3109/9781420020458

[2] Benjafield, A.V., Ayas, U.T., Eastwood, P.R., Heinzer, R., Ip, M.S.M., Morrell, M.J., Nunez, C.M., Patel, S.R., Penzel, T., Pépin, J.-L.D., 2019. Estimation of the global prevalence and burden of obstructive sleep apnoea: a literature-based analysis. Author manuscript. 7(8): 687–698. DOI : https://doi.org/10.1016/S2213-2600(19)30198-5

[3] Levitzky, M.G., 2008. Using the pathophysiology of obstructive sleep apnea to teach cardiopulmonary integration. Department of Physiology. New Orleans, Louisiana: Louisiana State University Health Sciences Center. 32: 196–202. DOI: https://doi.org/10.1152/advan.90137.2008

[4] Jehan, S., Zizi, F., Pandi-Perumal, S.R., Wall, S., Auguste, E., Myers, A.K., Jean-Louis, G., McFarlane, S.I., 2017. Obstructive Sleep Apnea and Obesity: Implications for Public Health. HHS Public Access. 1(4):93-99. DOI: https://doi.org/10.15406/smdij.2017.01.00019

[5] Wolk, R., Shamsuzzaman, A.S.M., Somers, V.K., 2003. Obesity, Sleep Apnea, and Hypertension. American Heart Association. 42:1067-1074. DOI: https://doi.org/10.1161/01.HYP.0000101686.98973.A3

[6] Chung, J., Lam, M., Choi, J., Mak, W., Sau, M., Ip, M., 2011. Obesity, obstructive sleep apnoea and metabolic syndrome. Asian Pacific Society of Respirology. 17: 223–236. DOI: https://doi.org/10.1111/j.1440-1843.2011.02081.x

[7] Godoy, I.R.B., Martinez-Salazar, E.L., Eajazi, A., Genta, P.R., Bredella, M.A., Torriani, M., 2016. Fat accumulation in the tongue is associated with male gender, abnormal upper airway measures and whole-body adiposity. HHS Public Access. 65(11): 1657–1663. DOI: https://doi.org/10.1016/j.metabol.2016.08.008.

[8] Wang, S.H., Keenan, B.T., Wiemken, A., Zang, Y., Staley, B., Sarwer, D.B., Torigian, D.A., Williams, N., Pack, A.I., Schwab, R.J., 2019. Effect of Weight Loss on Upper Airway Anatomy and the Apnea–Hypopnea Index. Respiratory and Critical Care Medicine. 201(6): 718–727 DOI: https://doi.org/10.1164/rccm.201903-0692OC

[9] Shang, Y., Hu, B., Yin, G., Fu, S., Ye, J., 2021. Computational fluid dynamics investigation on effects of uvulopalatopharyngoplasty on upper airway stability. AIP Advances. 11 (6): 065225. DOI: https://doi.org/10.1063/5.0053326

[10] Ogawa, T., Enciso, R., Shintaku, W.H., Clark, G.T., 2007. Evaluation of cross-section airway configuration of obstructive sleep apnea. NIH Public Access. 103(1), 102–108.DOI: https://doi.org/10.1016/j.tripleo.2006.06.008

[11] W.M.Faizal, Ghazali, N.N.N., Khor, C.Y., M.Z.Zainon, Ibrahim, N.B., Razif, R.M., 2021. Turbulent Kinetic Energy Of Flow During Inhale And Exhale To Characterize The Severity Of Obstructive Sleep Apnea Patient. Research Square. Version 1. DOI: https://doi.org/10.21203/rs.3.rs-1102041/v1

[12] Jeong, S.J., Kim, W.S., Sung, S.J., 2007. Numerical investigation on the flow characteristics and aerodynamic force of the upper airway of patient with obstructive sleep apnea using computational fluid dynamics. Medical Engineering & Physiccs. 29(2007): 637-651. DOI: https://doi.org/10.1016/j.medengphy.2006.08.017

[13] Mylavarapu, G., Murugappan, S., Mihaescu, M., Kalra, M., Khosla, S., Gutmark, E., 2009. Validation of computational fluid dynamics methodology used for human upper airway flow simulations. Journal of Biomech. 42: 1553-1559. DOI: https://doi.org/10.1016/j.jbiomech.2009.03.035

[14] Powell, N.B., Mihaescu, M., Mylavarapu, G., Weaver, E.M., Guilleminault, C., Gutmark, E., 2011. Patterns in pharyngeal airflow associated with sleep-disordered breathing. Sleep Medicine. 12: 966-974. DOI: https://doi.org/10.1016/j.sleep.2011.08.004

[15] M. Faizal, W., N. N. Ghazali, N., Y. Khor, C., Z. Zainon, M., Anjum Badruddin, I., Kamangar, S., Binti Ibrahim, N., Mohd Razi, R., 2021. Computational Analysis of Airflow in Upper Airway under Light and Heavy Breathing Conditions for a Realistic Patient Having Obstructive Sleep Apnea. Computer Modeling in Engineering & Sciences. 128: 583-604. DOI: https://doi.org/10.32604/cmes.2021.015549

[16] Riazuddin, V.N., Zubair, M., Abdullah, M.Z., Ismail, R., Shuaib, I.L., Hamid, S.A., Ahmad, K.A., 2010. Numerical Study of Inspiratory and Expiratory Flow in a Human Nasal Cavity. Journal of Medical and Biological Engineering. 31(3): 201-206. DOI: https://doi.org/10.5405/jmbe.781

[17] Li, L., Wu, W., Yan, G., Liu, L., Liu, H., Li, G., Li, J., Liu, D., 2016. Analogue simulation of pharyngeal airflow response to Twin Block treatment in growing patients with Class II1 and mandibular retrognathia. Scientific Reports. 6:26012. DOI: https://doi.org/10.1038/srep26012

[18] Issakhov, A., Mardieyeva, A., Zhandaulet, Y., Abylkassymova, A., 2021. Numerical study of air flow in the human respiratory system with rhinitis. Case Studies in Thermal Engineering. 26 (2001). DOI: https://doi.org/10.1016/j.csite.2021.101079

[19] Doorly, D.J., Taylor, D.J., Schroter, R.C., 2008. Respiratory Physiology & Neurobiology. Mechanics of airflow in the human nasal airway. 163 (2008) 100–110. DOI: https://doi.org/10.1016/j.resp.2008.07.027

[20] Park, S.B., Khattar, D., 2022. Tachypnea. Treasure Island (FL): StatPearls Publishing. PMID: 31082106

[21] Suga, H., Iwasaki, T., Mishima, K., Nakano, H., Ueyama, Y., Yamasaki, Y., 2021. Evaluation of the effect of oral appliance treatment on upper-airway ventilation conditions in obstructive sleep apnea using computational fluid dynamics. Cranio. 39(3): 209-217. DOI: https://doi.org/10.1080/08869634.2019.1596554

[22] Ahookhosh, K., Saidi, M., Aminfar, H., Mohammadpourfard, M., Hamishehkar, H., Yaqoubi, S., 2020. Dry powder inhaler aerosol deposition in a model of tracheobronchial airways: Validating CFD predictions with in vitro data. International Journal of Pharmaceutics. 587 (2020) 119599. DOI: https://doi.org/10.1016/j.ijpharm.2020.119599

[23] Srivastav, V.K., Paul, A.R., Jain, A., 2019. Capturing the wall turbulence in CFD simulation of human respiratory tract. Mathematics and Computers in Simulation. 160: 23-38. DOI: https://doi.org/10.1016/j.matcom.2018.11.019

[24] Cai, H., Xu, C., Xue, H., Guo, Y., Su, L., Gao, X., 2022. Upper airway flow characteristics of childhood obstructive sleep apnea-hypopnea syndrome. Scientific Reports. 12(2022): 7386. DOI: https://doi.org/10.1038/s41598-022-10367-w

[25] Bates, A.J., Doorly, Cetto, R., Calmet, H., Gambaruto, A.M., Tolley, N.S., Houzeaux, G., Schroter, R.C., 2014. Dynamics of airflow in a short inhalation. Bioengineering, biomedical engineering,biomechanics. 12: 20140880. DOI: http://dx.doi.org/10.1098/rsif.2014.0880

[26] Wang, L., Ge, H., Chen, L., Hajipour, A., Feng, Y., Cui, X., 2021. LES study on the impact of airway deformation on the airflow structures in the idealized mouth–throat model. Journal of the Brazilian Society of Mechanical Sciences and Engineering. 44(2022): 23 DOI: https://doi.org/10.1007/s40430-021-03324-7

[27] Guo, Y., Wei, J., Ou, C., Liu, L., Sadrizadeh, S., Jin, T., Tang, L., Zhang, Y., Li, Y., 2020. Deposition of droplets from the trachea or bronchus in the respiratory tract during exhalation: A steady-state numerical investigation. Aerosol Science and Technology. 54(8): 869-879 DOI: https://doi.org/10.1080/02786826.2020.1772459